PROCEEDINGS OF SCIENCE

Search for heavy Higgs bosons A/H decaying to a top quark pair in pp collisions at $\sqrt{s} = 8$ TeV with the ATLAS detector

Janna Katharina Behr*
On behalf of the ATLAS Collaboration

Deutsches Elektronen-Synchrotron, Notkestr. 85, 22607 Hamburg
E-mail: katharina.behr@cern.ch

A search for heavy pseudoscalar (A) and scalar (H) Higgs bosons decaying into a top quark pair ($t\bar{t}$) has been performed with 20.3 fb^{-1} of proton–proton collision data collected by the ATLAS experiment at the Large Hadron Collider at a center-of-mass energy of $\sqrt{s} = 8$ TeV. Interference effects between the signal process and Standard Model $t\bar{t}$ production, which are expected to distort the signal shape from a single peak to a peak–dip structure, are taken into account. No significant deviation from the Standard Model prediction is observed in the $t\bar{t}$ invariant mass spectrum in final states with an electron or muon, large missing transverse momentum, and at least four jets. The results are interpreted within the context of a type-II two-Higgs-doublet model. Exclusion limits on the signal strength are derived as a function of the mass $m_{A/H}$ and the ratio of the vacuum expectation values of the two Higgs fields, $\tan\beta$, for $m_{A/H} > 500$ GeV.

EPS-HEP 2017, European Physical Society conference on High Energy Physics
5-12 July 2017
Venice, Italy

*Speaker.

PoS(EPS-HEP2017)259

1. Introduction

Additional Higgs bosons are predicted by many extensions of the Standard Model (SM), including supersymmetry and models of dark matter. The search for these extra Higgs bosons is among the primary physics goals of the experiments at the Large Hadron Collider (LHC). In many of these models, the SM Higgs sector is extended to contain a second Higgs doublet. Two-Higgs doublet models (2HDMs) predict the existence of five physical Higgs bosons. Their decays depend on the parameters of the 2HDM such that searches in different final states cover complementary parameter regions.

In this contribution, the first search for the heavy scalar (H) and pseudoscalar (A) Higgs bosons of a 2HDM in final states with a top-antiop pair ($t\bar{t}$) is presented, summarising the recent results of Ref. [1] on 20.3 fb^{-1} of proton-proton collision data at a centre-of-mass energy $\sqrt{s} = 8$ TeV, collected by the ATLAS experiment [2]. The key challenge for searches in this final state is the strong interference between the signal process, gluon–gluon (gg) initiated loop production of A or H, and the irreducible background from SM $t\bar{t}$ production. The resulting signal shape is distorted from a Breit–Wigner peak to a peak–dip structure. Previous searches for $t\bar{t}$ resonances [3, 4], which aimed to identify local resonant excesses in the $t\bar{t}$ invariant mass ($m_{t\bar{t}}$) spectrum, have a reduced sensitivity to these signal processes.

The analysis results are interpreted in the context of a type-II 2HDM with a softly broken Z_2 symmetry [5], assuming that the ligher of the two CP-even states, h, is the Higgs boson discovered at a mass of $m_h = 125$ GeV with couplings as predicted by the SM. This corresponds to the condition $\sin(\alpha - \beta) = 1$, referred to as the *alignment limit*, where α denotes the mixing angle between the two CP-even states. The parameter m_{12} of the Z_2 breaking term of the potential is taken to be $m_{12}^2 = m_A^2 \tan\beta/(1+\tan^2\beta)$. The production cross-sections and widths of A and H, and the signal shape, are then fully determined by $\tan\beta$ and the masses m_A and m_H. Three mass hierarchies are considered. In the first two scenarios, one of the Higgs bosons is significantly heavier than the other such that only the interference pattern of the lighter boson appears in the $m_{t\bar{t}}$ spectrum. In the last scenario, A and H are assumed to be mass degenerate ($m_H = m_A$) such that both processes contribute to the $m_{t\bar{t}}$ spectrum.

2. Analysis Strategy

The analysis is based upon the resolved-topology analysis in Ref. [3]. Events with signatures compatible with $t\bar{t} \to W^+bW^-\bar{b}$, with one W boson decaying hadronically and the other leptonically, are selected using single-electron and -muon triggers. Details of the event selection and reconstruction are given in Ref. [3]. The dominant background process is SM $t\bar{t}$ production, followed by W+jets production. Monte Carlo (MC) generators are used to simulate the signal and all background processes, the only exceptions being the normalisation of the W+jets background contribution and the estimate of the contribution from multijets production, which are obtained using data-driven techniques. The background estimates for all processes are identical to those used in Ref. [3]. In particular, SM $t\bar{t}$ production was simulated at next-to-leading order (NLO) with POWHEG-BOX [6, 7, 8, 9] + PYTHIA6 [10].

3. Signal Modelling

The model of Ref. [11] within MADGRAPH5_aMC@NLO [12] v2.3.3 was used to simulate the signal process $gg \to A/H \to t\bar{t}$, including the decays of the top quarks and resulting W bosons, with loop contributions from top and bottom quarks at leading order in QCD. The MADGRAPH5_aMC@NLO software was modified to remove the pure SM $t\bar{t}$ process to yield only the signal-plus-interference $S+I$ contribution on an event-by-event basis. In addition, pure signal samples S were generated. The parton shower and hadronisation were modelled with PYTHIA6 and the resulting stable particles were passed through the ATLAS fast detector simulation [13]. The effects of additional collisions within the same or nearby bunch crossings were simulated by overlaying additional pp collisions, simulated with PYTHIA v8.1 [14], on each event. Correction factors were applied to adjust the trigger and selection efficiencies in simulated events to those measured in data.

An event-by-event reweighting method was used to obtain S and $S+I$ samples with varying values of $(m_{A/H}, \tan\beta)$ from signal samples S after the detector simulation. Signal hypotheses with $m_{A/H} < 500$ GeV were not studied as they require the implementation of higher-order corrections and an accurate modeling of the Higgs boson decay into virtual top quarks that are not implemented in the current model. The requirement $\tan\beta \geq 0.4$ was imposed to ensure that all amplitudes involving scalars preserve perturbative unitarity [5].

Correction factors K_S were applied to normalize the generated signal cross-section to the cross-section calculated at partial next-to-next-to-leading-order (NNLO) precision in QCD. The correction factor for the interference component I is $K_I = \sqrt{K_S \times K_B}$, where $K_B = 1.87$ [1].

4. Systematic Uncertainties

The experimental uncertainties with the largest impact on the normalisation and shape of the $m_{t\bar{t}}^{\text{reco}}$ distributions are those related to the jet energy scale and the jet energy resolution. The largest theoretical uncertainty on the background modelling is the 6.5% uncertainty on the cross-section for SM $t\bar{t}$ production, calculated at NNLO accuracy in QCD, including resummation of next-to-next-to-leading-logarithmic soft gluon terms. Further uncertainties are related to the choice of NLO event generator, the modeling of the parton shower and fragmentation, the modeling of gluon initial- and final-state radiation, and the value of the top quark mass m_t. A detailed description of the different sources of uncertainty related to the various background components can be found in Ref. [3].

The dominant uncertainty in the modeling of the $S+I$ and S components is related to the ± 1.0 GeV uncertainty of the value $m_t = 172.5$ GeV. Furthermore, uncertainties related to the choice of PDF set and renormalization and factorization scales are considered. The latter uncertainty is obtained by varying the scales by factors of 0.5 and 2.0, which yields a constant $\pm 7.3\%$ variation across the $m_{t\bar{t}}^{\text{reco}}$ spectrum. An asymmetric variation, for which the bins at the low and high ends of the $m_{t\bar{t}}^{\text{reco}}$ spectrum are taken as anticorrelated [15] is also taken into account to estimate the impact of the scale variations on the shape of the $m_{t\bar{t}}^{\text{reco}}$ spectrum. An additional constant $\pm 5\%$ uncertainty is included for the $S+I$ samples to cover the difference between reweighted and generated distributions.

5. Results

Each signal hypothesis is tested using a profile likelihood fit of the expected $m_{t\bar{t}}^{\text{reco}}$ distributions to the observed ones simultaneously in all signal regions. The statistical and systematic uncertainties are taken into account as nuisance parameters. The shape of the binned $m_{t\bar{t}}^{\text{reco}}$ distributions in the presence of interference is parameterised in terms of the signal strength μ:

$$\mu \cdot S + \sqrt{\mu} \cdot I + B = (\mu - \sqrt{\mu}) \cdot S + \sqrt{\mu} \cdot (S + I) + B. \tag{5.1}$$

The case $\mu = 1$ corresponds to the type-II 2HDM in the alignment limit. The terms S and $S+I$ on the right-hand side of Eq. (5.1) correspond to the $m_{t\bar{t}}^{\text{reco}}$ distributions obtained from the S and $S+I$ samples, respectively, while B stands for the expected $m_{t\bar{t}}^{\text{reco}}$ distribution of the total SM background. Only bins with $m_{t\bar{t}}^{\text{reco}} > 320$ GeV are considered in the fit to avoid threshold effects that are not well described by the simulation.

The agreement between the observed and expected mass spectra is quantified in a fit under the background-only hypothesis ($\mu = 0$). In Figure 1, the observed and expected $m_{t\bar{t}}^{\text{reco}}$ spectra are shown. Observed and expected spectra are in good agreement within the (constrained) uncertainty bands.

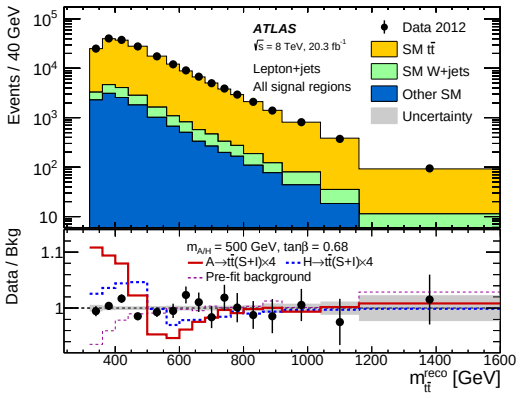

Figure 1: Observed and expected distributions of $m_{t\bar{t}}^{\text{reco}}$ after the profile-likelihood fit under the background-only hypothesis. All signal regions are combined. In the bottom panel, the $S+I$ distributions (scaled by a factor of four) for a pseudoscalar A (solid) and scalar H (bold dashed) with $m_{A/H} = 500$ GeV and $\tan\beta = 0.68$ are shown relative to the total expected background. The last bin includes overflow events. Taken from Ref. [1].

The upper limit on μ for each signal hypothesis, at 95% confidence level (CL), is derived with the CL_S method. Exclusion limits at intermediate points in the $(m_{A/H}, \tan\beta)$ plane are obtained from a linear interpolation among the three closest points. In Figure 2, the observed and expected exclusion regions for the type-II 2HDM ($\mu = 1$) are shown for the three mass hierarchies discussed in the introduction.

6. Summary

No statistically significant deviations from the SM prediction is found in the search for heavy Higgs bosons A/H decaying to $t\bar{t}$ in 20.3 fb^{-1} of pp collisions data at 8 TeV recorded by the

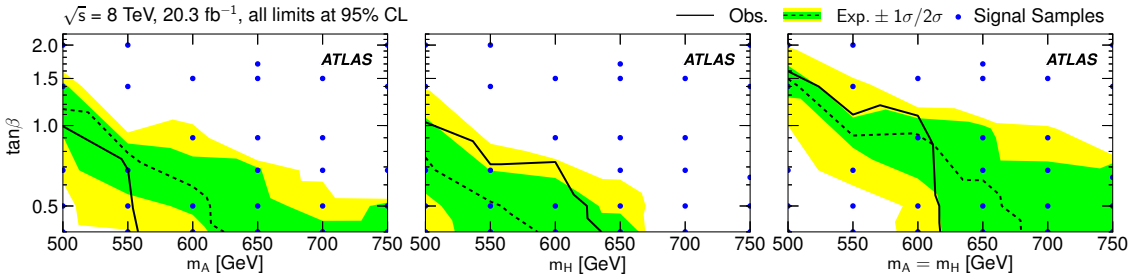

Figure 2: The 95% CL observed and expected exclusion regions for the type-II 2HDM ($\mu = 1$) considering only a pseudoscalar A (left), only a scalar H (middle), and the mass-degenerate scenario $m_A = m_H$ (right). The areas below the solid (dashed) lines are observed (expected) to be excluded. Blue points indicate parameter values at which signal samples are produced. Values at intermediate points are obtained from a linear triangular interpolation among the three closest points. Taken from Ref. [1].

ATLAS experiment. The analysis results are interpreted in a type-II 2HDM in the alignment limit, and upper limits are quoted on the signal strength μ at 95% CL in the $m_{A/H} - \tan\beta$ plane. The search presented in this contribution is the first search for massive resonances in $t\bar{t}$ final states that takes into account interference effects between the signal process and the background from SM $t\bar{t}$ production. It provides the first direct constraints in the parameter region with $m_{A/H} > 500$ GeV and low $\tan\beta$.

References

[1] ATLAS Collaboration, [arXiv:1707.06025 [hep-ex]]. Submitted to PRL.

[2] ATLAS Collaboration, JINST **3** (2008) S08003.

[3] ATLAS Collaboration, JHEP **1508** (2015) 148 [arXiv:1505.07018 [hep-ex]].

[4] CMS Collaboration, JHEP **1707** (2017) 001 [arXiv:1704.03366 [hep-ex]].

[5] J. F. Gunion and H. E. Haber, Phys. Rev. D **67** (2003) 075019 [hep-ph/0207010].

[6] S. Frixione, P. Nason and G. Ridolfi, JHEP **0709** (2007) 126 [arXiv:0707.3088 [hep-ph]].

[7] P. Nason, JHEP **0411** (2004) 040 [hep-ph/0409146].

[8] S. Frixione, P. Nason and C. Oleari, JHEP **0711** (2007) 070 [arXiv:0709.2092 [hep-ph]].

[9] S. Alioli, P. Nason, C. Oleari and E. Re, JHEP **1006** (2010) 043 [arXiv:1002.2581 [hep-ph]].

[10] T. Sjostrand, S. Mrenna and P. Z. Skands, JHEP **0605** (2006) 026 [hep-ph/0603175].

[11] Buarque Franzosi, D. and Zhang, C., https://cp3.irmp.ucl.ac.be/projects/madgraph/wiki/Models/ggHFullLoop

[12] J. Alwall *et al.*, JHEP **1407** (2014) 079 [arXiv:1405.0301 [hep-ph]].

[13] ATLAS Collaboration, ATL-PHYS-PUB-2010-013,

[14] T. Sjostrand, S. Mrenna and P. Z. Skands, Comput. Phys. Commun. **178** (2008) 852 [arXiv:0710.3820 [hep-ph]].

[15] J. M. Lindert *et al.*, arXiv:1705.04664 [hep-ph].